HHS Public Access

Author manuscript

Nat Struct Mol Biol. Author manuscript; available in PMC 2015 April 04.

Published in final edited form as:

Nat Struct Mol Biol. 2015 April ; 22(4): 328–335. doi:10.1038/nsmb.2979.

Small-RNA loading licenses Argonaute for assembly into a transcriptional silencing complex

Daniel Holoch and **Danesh Moazed**

Department of Cell Biology, Howard Hughes Medical Institute, Harvard Medical School, Boston, Massachusetts, USA

Abstract

Argonautes and their small-RNA cofactors form the core effectors of ancient and diverse gene-silencing mechanisms whose roles include regulation of gene expression and defense against foreign genetic elements. Although Argonautes generally act within multisubunit complexes, what governs their assembly into these machineries is not well defined. Here, we show that loading of small RNAs onto Argonaute is a checkpoint for Argonaute's association with conserved GW-protein components of silencing complexes. We demonstrate that the Argonaute small interfering RNA chaperone (ARC) complex mediates loading of small RNAs onto Ago1 in *Schizosaccharomyces pombe* and that deletion of its subunits, or mutations in Ago1 that prevent small-RNA loading, abolish the assembly of the GW protein–containing RNA-induced transcriptional silencing (RITS) complex. Our studies uncover a mechanism that ensures that Argonaute loading precedes RITS assembly and thereby averts the formation of inert and potentially deleterious complexes.

Small silencing RNA molecules represent an ancient and widespread strategy for regulating gene expression and protecting the genome from foreign and unstable DNA elements[1–4]. Small RNAs drive sequence-specific silencing by guiding proteins of the conserved Argonaute family. Argonautes inactivate their targets by endonucleolytic cleavage or by recruiting additional factors to mediate translational repression, RNA turnover or transcriptional silencing through chromatin modification of the corresponding loci[5–7]. In most cases, Argonautes function within multisubunit assemblies called the RNA-induced silencing complex (RISC) or, in the nucleus, the RITS complex[8,9]. The mechanisms that control the formation of these protein complexes are not well understood.

Correspondence should be addressed to D.M. (danesh@hms.harvard.edu).

Accession codes. The raw and processed small-RNA data have been deposited in the Gene Expression Omnibus database under accession number GSE65223. The deposited processed data can be visualized with the Integrative Genomics Viewer (http://www.broadinstitute.org/igv/).

Note: Any Supplementary Information and Source Data files are available in the online version of the paper.

AUTHOR CONTRIBUTIONS

D.H. and D.M. designed the study. D.H. performed all experiments and bioinformatic analysis. D.H. and D.M. analyzed the data and wrote the paper.

COMPETING FINANCIAL INTERESTS

The authors declare no competing financial interests.

In the fission yeast *S. pombe*, small RNAs mediate silencing at the transcriptional level. The Argonaute-containing RITS complex is recruited to nascent transcripts at the *dg* and *dh* noncoding repeats, which flank the centromeres of each chromosome, by endogenous small interfering RNAs (siRNAs), whose biogenesis requires the Dicer family RNase Dcr1 (refs. 9–12). Because siRNAs are initially generated as duplexes, endonucleolytic cleavage of the 'passenger' strand by the 'slicer' activity of Argonaute, and its release, must occur before the remaining 'guide' strand can mediate recognition of pericentromeric nascent transcripts[13–15]. Once recruited, siRNA-programmed RITS directs heterochromatic silencing of the *dg* and *dh* repeats via methylation of nucleosomes on histone H3 Lys9 (H3K9) by the Clr4–Rik1–Cul4 (CLRC) complex[9,16–20]. Pericentromeric heterochromatin is important for accurate chromosome segregation and maintenance of genomic stability in *S. pombe*[21,22], a requirement widely shared among multicellular eukaryotes[23].

The RITS complex contains Chp1 (a chromodomain protein) and Tas3 (a member of the conserved Gly-Trp (GW) motif–containing family[9]) in addition to the single *S. pombe* Argonaute protein Ago1 (Fig. 1a). Tas3 orthologs bind to Argonautes via their GW or 'Ago-hook' domains and participate in different modes of small RNA–mediated silencing in a broad range of organisms[9,24–32]. Through extensive mutagenesis studies, the GW domain–recognition site has been mapped to a region spanning the MID and PIWI domains of Argonaute, in particular to amino acid residues crucial for anchoring the 5′-monophosphate end of the guide small RNA[27,33]. Accordingly, some groups have suggested that a relationship exists between the loading of Argonaute with a guide RNA and its association with GW domains, whereas other studies have contended that the activities are separable[34–37]. Association of unloaded Argonautes with GW proteins and downstream factors might be expected to generate inactive complexes that poison the activity of mature small RNA–programmed complexes and their own ability to interact with downstream factors. Although studies have been carried out with overexpressed proteins[36,37], it is currently unknown whether the interaction of endogenous Argonaute with GW proteins depends on small-RNA loading or is regulated by other mechanisms.

Previously, we reported the discovery of a distinct Ago1-containing complex in fission yeast, called the ARC complex, which includes Arb1, a protein present throughout the fungal lineage that bears homology to organellar maturases, and Arb2, which is broadly conserved in fungi, plants and metazoans but whose function is unknown[13]. Immunofluorescence assays have shown ARC to be localized to the nucleus, but MS analyses have indicated that RITS and ARC are distinct complexes with only the Ago1 subunit in common[9,13]. ARC carries duplex siRNAs and, despite its nuclear localization, appears not to associate with chromatin, thus suggesting that, in contrast to RITS, it is not directly involved in target-transcript engagement[13,38]. An explanation for the observation that ARC-associated siRNAs are double-stranded has come from the finding that Arb1 inhibits Ago1 slicer activity and thus passenger-strand release[13]. Alone, this result might imply that ARC acts as a negative modulator of the siRNA pathway, but on the contrary ARC has a critical positive role in siRNA-directed heterochromatin assembly because deletions of *arb1*$^{+}$ and *arb2*$^{+}$ cause a similar loss of pericentromeric H3K9 methylation and

gene silencing as deletion of *ago1*$^{+}$ (ref. 13). However, the specific nature of their contribution to siRNA-dependent heterochromatin formation has remained undefined.

In this study, we set out to determine the role of ARC in gene silencing. We identify ARC as the machinery responsible for siRNA loading in *S. pombe* and demonstrate that this loading activity is required for assembly of the RITS complex. Premature assembly of Argonautes lacking small-RNA guides into effector complexes, such as RITS, is expected to result in undesired competition for limiting downstream silencing factors. The ordered assembly pathway described here is therefore likely to be a central and conserved feature of the mechanisms that regulate the association of Argonautes with their GW-protein partners.

RESULTS

Arb1 and Arb2 are required for assembly of the RITS complex

It has been presumed that individual Ago1 molecules begin their life cycle in ARC before undergoing a transition to the RITS complex. We therefore asked whether Ago1 retains the ability to be assembled into RITS when its passage through ARC is prevented by genomic deletion of *arb1*$^{+}$ or *arb2*$^{+}$. Surprisingly, we found that the interaction between Ago1 and the GW protein Tas3 was abolished in *arb1*Δ and *arb2*Δ cells (Fig. 1b). Importantly, a considerable degree of interaction persisted in *dcr1*Δ cells[9]. This indicates that the loss of heterochromatic silencing common to *dcr1*Δ, *arb1*Δ and *arb2*Δ cells is not sufficient to explain the loss of RITS integrity. Instead, the data suggest that Arb1 and Arb2 license Ago1 for entry into RITS by an unknown mechanism. We also used coimmunoprecipitation to monitor the integrity of ARC in cells lacking Tas3. We found that, in contrast to the effect of ARC on RITS assembly, the association between ARC subunits Ago1 and Arb1 was enhanced in *tas3*Δ as well as in *dcr1*Δ cells and was not diminished in *arb2*Δ cells (Fig. 1c). Mixture MS analysis of triple Flag-tagged (3×Flag) Ago1 purifications from wild-type and *tas3*Δ cells confirmed that Ago1-Arb1 and Ago1-Arb2 interactions remained intact in the absence of the RITS complex (Supplementary Fig. 1). Together these results show that Ago1 can assemble with Arb1 and Arb2 into the ARC complex independently of RITS, but Ago1 can enter the RITS complex only after passage through ARC.

Small-RNA loading of Argonaute is required for RITS assembly

The altered interactions within each of the two Argonaute complexes in *dcr1*Δ cells were striking and suggestive of a relationship between small-RNA levels and complex assembly. We therefore hypothesized that loading of a small RNA onto Ago1 is a prerequisite for RITS assembly and that Arb1 and Arb2 are required for entry of Ago1 into RITS because they mediate this activity. Importantly, *S. pombe* cells produce a class of Dicer-independent small RNAs, called primal RNAs (priRNAs), whose biogenesis requires the exonuclease Triman and which can direct H3K9 methylation in an Argonaute-dependent manner[39,40]. Therefore, the maintenance of RITS in *dcr1*Δ cells might reflect loading of Argonaute with these remaining small RNAs, and it is compatible with a model in which RITS assembly is strictly contingent on a small RNA–binding event.

In order to test this model directly, we generated a mutant of Ago1 that cannot load small RNAs and asked whether it would associate with the GW protein Tas3 *in vivo*. A mutagenesis study by Till *et al.*[27] showed that the region of human Argonaute2 required for recognition by the GW protein TNRC6B corresponds to MID- and PIWI-domain residues identified in structural studies to be involved in anchoring the monophosphorylated 5′ end of the guide RNA[41]. We therefore needed to leave the equivalent *S. pombe* residues (Y513 and K517) intact. Instead, we combined a previously used PAZ-domain mutation (F276A), which impairs binding of the guide-RNA 3′ end but only partially reduces loading *in vivo*[13,31,42], with a mutation in a conserved arginine (R773E) shown in a recent crystal structure of full-length human Argonaute2 to make electrostatic contacts with two phosphates in the small-RNA backbone[43] (Fig. 2a). Mutation of the corresponding arginine by itself does not disrupt *in vitro* binding of Argonaute2 to TNRC6B, thus suggesting that this residue does not directly contact GW-domain proteins[27]. We integrated 3×Flag-tagged wild-type and mutant alleles at an ectopic site near the *trp1*$^+$ gene[44] (Supplementary Fig. 2a). A wild-type 3×Flag-*ago1* insertion at this locus rescued *ago1*Δ in silencing of a pericentromeric *ura4*$^+$ reporter gene (Supplementary Fig. 2b). Similarly to the previously studied slicer-dead mutant *ago1* D580A (refs. 13,45), *ago1* F276A R773E failed to complement *ago1*Δ, but neither allele was dominant negative at single copy number. Moreover, total pericentromeric *dg* siRNA levels were unperturbed by these alleles when *ago1*$^+$ was also present (Supplementary Fig. 2c). Importantly, no *dg* siRNAs copurified with Ago1 F276A R773E, despite their normal abundance in total cellular RNA, thus demonstrating that the mutant protein is unable to load small RNAs. We also generated strains expressing the single-mutant proteins Ago1 F276A or Ago1 R773E. Although neither restored pericentromeric reporter silencing in *ago1*Δ, only Ago1 R773E was fully deficient for *dg* siRNA loading, whereas Ago1 F276A retained some loading activity, as had been observed previously upon overexpression of this allele[13]. In agreement with earlier results, Ago1 D580A associated with slightly longer siRNAs, thus suggesting that passenger-strand release coincides with an exonucleolytic trimming event[39].

Consistently with the hypothesis that loading of a small RNA onto Ago1 is a prerequisite for its assembly into RITS, we detected no association between Tas3 and either Ago1 F276A R773E or Ago1 R773E (Fig. 2b and Supplementary Fig. 2d). In contrast, the null-mutant protein Ago1 D580A, which loads duplex siRNAs but cannot release the siRNA passenger strand[13], was still incorporated into RITS, as was another null protein that nevertheless can load siRNAs, Ago1 F276A. Recent studies have shown that Argonaute protein stability is affected by small-RNA availability in different organisms[46,47]. In agreement with these reports, Ago1 F276A R773E and Ago1 R773E were also present at reduced levels in whole cell extracts. However, this does not account for their failure to associate with Tas3 because they associated with Arb1 at levels comparable to those observed in the wild-type variant (Fig. 2c and Supplementary Fig. 2e). We conclude that small-RNA loading onto Ago1 is a precondition for its assembly into RITS but not ARC.

ARC-associated small RNAs bear features of Dicer products

The requirement for *arb1*$^+$, *arb2*$^+$ and small-RNA loading in RITS-complex assembly suggests that ARC may regulate RITS assembly by loading small RNAs onto Ago1. To test

this hypothesis, we first determined the nature of small RNAs bound to RITS and ARC *in vivo* by purifying RNA associated with tandem affinity purification (TAP)-tagged Tas3-TAP and TAP-Arb1, respectively, and performing northern blot analysis. Confirming previous results[13], a non-denaturing northern blot showed that *dg* siRNAs bound to ARC were double-stranded, suggesting that ARC binds duplex siRNAs generated by Dcr1 (Fig. 3a, lane 6). Intriguingly, a denaturing blot showed that the ARC-bound *dg* siRNAs were longer than those bound to RITS (Fig. 3b, comparison of lanes 5 and 6). This is consistent with the idea that they are products of the Dicer RNase, which in *S. pombe* lacks a PAZ domain and consequently produces siRNAs of varying sizes that are subsequently pared by exonucleolytic trimming[10,39,40]. We next examined small RNAs bound to Tas3-TAP and TAP-Arb1 by high-throughput sequencing and found similar populations of pericentromeric reads in the two libraries (Supplementary Table 1 and Supplementary Fig. 3). A plot of their length distributions showed that siRNAs mapping throughout the *dg* and *dh* repeats were indeed longer, and displayed a broader size distribution, when bound to ARC rather than to RITS (Fig. 3c). Finally, a considerable fraction of *dg* and *dh* small-RNA reads from the ARC library did not begin with the 5′-uridine typical of Ago1 guide RNAs, unlike their RITS counterparts (Fig. 3d), a result suggestive of the presence of siRNA passenger strands in ARC.

Arb1 is required for loading Argonaute with small RNAs

The data above support the idea that the products of Dcr1 are loaded onto ARC but do not clarify whether Arb1 and Arb2 are required for loading. In order to address this question, we developed an *in vitro* small-RNA binding assay, using immunopurified proteins bound to magnetic beads. First we compared binding of immobilized RITS and ARC complexes to single-stranded and duplex RNAs (Fig. 4a). In order to increase the recovery of Ago1 molecules not already bound to small RNAs, we purified Ago1 from *dcr1*Δ cells. We confirmed that Tas3-TAP and TAP-Arb1 purifications coprecipitated 3×Flag-tagged Ago1 with specificity (Supplementary Fig. 4a) and adjusted these RITS and ARC preparations with untreated beads to normalize for Ago1 content (Fig. 4b). We then radiolabeled a single-stranded 22-nt RNA and a 22-bp duplex RNA with 2-nt 3′ overhangs—a signature of Dicer-generated siRNAs—and verified their purity (Supplementary Fig. 4b). We incubated these RNAs with each complex and with beads from a mock purification, washed away unbound material and visualized the remaining RNA by denaturing gel electrophoresis. Although both complexes retained the single-stranded species, only ARC was able to load duplex small RNAs (Fig. 4c, comparison of lanes 6 and 8, and Fig. 4d). Consistently with the coimmunoprecipitation data above, these results suggest that loading of double-stranded Dicer products onto Argonaute must precede RITS formation because this activity was lost once the complex was assembled.

In principle, when not in RITS, Argonaute could exist within the ARC complex or as a free protein and might load duplex small RNAs in either situation. In order to determine whether the activity is mediated by ARC or is simply inhibited by the other RITS subunits, we performed binding assays using total immunopurified 3×Flag-Ago1 (Fig. 4e). Western blot analysis of the magnetic beads showed varying stabilities for Ago1 from different backgrounds (Fig. 4f and Supplementary Fig. 4c). However, the binding assay showed that,

in contrast to Ago1 isolated from wild-type cells, Ago1 isolated from *tas3*Δ *arb1*Δ or *arb1*Δ cells was incapable of loading duplex small RNAs (Fig. 4g, comparison of lanes 3–5, and Fig. 4h). We therefore conclude that Ago1 outside of the RITS and ARC complexes bears no duplex siRNA–loading activity and consequently that duplex siRNA loading strictly requires Arb1. Further supporting this model, Ago1 isolated from *tas3*Δ cells, although no more abundant than that from *tas3*Δ *arb1*Δ cells, exhibited excellent loading activity. We found that the duplex siRNA–loading activity of Ago1 purified from *arb2*Δ cells, in contrast to that of Ago1 purified from *arb1*Δ cells, was similar to that of Ago1 purified from wild-type cells (Supplementary Fig. 4d, comparison of lanes 3–5, and Supplementary Fig. 4e). Thus, an Arb1–Ago1 subcomplex is sufficient for duplex-small-RNA loading in our assay, and indeed Arb1 and Ago1 remain stably associated in *arb2*Δ cells.

In contrast to *arb1*Δ cells, *dcr1*Δ cells have a mild RITS-assembly defect, thus suggesting that Dcr1-independent single-stranded priRNAs might be loaded onto Ago1 in an Arb1-dependent manner. We tested this hypothesis by performing high-throughput sequencing of Ago1-bound small RNAs isolated from *dcr1*Δ, *arb1*Δ and *dcr1*Δ *arb1*Δ cells. We had previously observed that pericentromeric siRNAs were only modestly reduced in *arb1*Δ cells[39], a result seemingly at odds with the notion that Arb1 is required for Ago1 loading. However, we had obtained this result with overexpressed Ago1, and we present evidence below that *ago1*$^{+}$ acts as a high-dosage suppressor of *arb1*Δ and *arb2*Δ with respect to siRNA generation, which in fact is normally lost in these mutants. Therefore, we reasoned that in cells expressing endogenous levels of Ago1, Arb1 may indeed be required for all small-RNA loading. To assess the background of contaminating cellular small RNAs in our purifications, we also constructed a library by using a 3×Flag-tagged Ago1 variant with amino acid substitutions that compromise loading of small RNAs into the canonical binding groove (F276A Y513A K517A, hereafter referred to as Ago1 3A)[39]. We coexpressed this allele and an untagged wild-type *ago1*$^{+}$ allele in order to maintain abundant levels of pericentromeric siRNAs and to verify that these did not copurify with Ago1 3A.

We found that pericentromeric siRNAs bound to endogenous Ago1 were severely reduced in *arb1*Δ cells compared to wild-type cells, to levels similar to those observed in *dcr1*Δ and *dcr1*Δ *arb1*Δ cells and even lower than the Ago1 3A–associated background (Fig. 5a–c and Supplementary Note). Therefore, in contrast to overexpressed Ago1 (ref. 39), Ago1 expressed at endogenous levels does not associate with small RNAs mapping to the *dg* and *dh* repeats in cells lacking Arb1.

In order to determine whether Arb1 is required for loading Dcr1-independent single-stranded priRNAs *in vivo*, we used general characteristics of the reads to distinguish between genuine loading events and nonspecific recovery of small RNAs in 3×Flag-Ago1 immunoprecipitations. The small-RNA guides of each Argonaute homolog exhibit specific lengths as well as a 5′ nucleotide bias conferred by the structure of the 5′ end–binding pocket[7,48]. *S. pombe* Ago1 binds small RNAs of 22 to 23 nt beginning with a 5′-uridine[49]. As we have observed previously[39], the Ago1-bound small RNAs in *dcr1*Δ cells, although depleted in pericentromeric sequences, exhibited the same narrow peak of 22-nt and 23-nt reads and the same overwhelming 5′-uridine preference as the small RNAs bound to Ago1 in wild-type cells (Fig. 5d,e). This indicates that they represent bona fide guide molecules

loaded into the small RNA–binding channel of Argonaute. In contrast, the length distributions of the Ago1-associated small RNAs from *arb1*Δ and *dcr1*Δ *arb1*Δ cells were very broad, strongly resembling that observed for the background small RNAs associating with Ago1 3A. Similarly, the frequency of reads with 5′-uridines was dramatically lowered in the *arb1*Δ and *dcr1*Δ *arb1*Δ libraries, nearly to the extent observed in the Ago1 3A library. These results demonstrate that Arb1 is required for loading both Dcr1-dependent duplex siRNAs and Dcr1-independent single-stranded priRNAs into Ago1 *in vivo*.

Ago1 overexpression partially overcomes *arb1*Δ loading defect

As noted above, pericentromeric siRNA levels in Arb1-deficient cells differ considerably, depending on whether Ago1 is present at endogenous or overexpressed levels. We found that, in addition to rescuing siRNA accumulation, *ago1*$^+$ overexpression suppressed the silencing defect of a pericentromeric reporter transgene (*otr1R::ura4*$^+$) in *arb1*Δ and *arb2*Δ cells (Fig. 6a). However, the noncoding transcripts from the *dg* and *dh* repeats remained partially derepressed under these conditions, thus suggesting that *ago1*$^+$ overexpression did not fully restore silencing in *arb1*Δ and *arb2*Δ cells (Fig. 6b). Pericentromeric H3K9 dimethylation, normally lost in *arb1*Δ and *arb2*Δ cells, was fully recovered by the action of overexpressed Ago1 (Fig. 6c). A northern blot analysis of siRNAs mapping to the *dg* and *dh* repeats confirmed our previous sequencing work using overexpressed *ago1*$^+$, showing robust recovery of *dg* siRNAs and only partial restoration of *dh* siRNAs in *arb1*Δ and *arb2*Δ cells[39] (Fig. 6d and Supplementary Note). Finally, hypersensitivity to the microtubule poison thiabendazole, which occurs in mutants without pericentromeric heterochromatin because of defects in chromosome segregation, was suppressed in *arb1*Δ and *arb2*Δ when *ago1*$^+$ was overexpressed, thus suggesting that the heterochromatin restored in these cells was functional (Fig. 6e).

Although overexpression from our construct was between 50 and 100 times endogenous levels (Supplementary Fig. 5a), Ago1 protein accumulation was only modestly affected in *arb1*Δ and *arb2*Δ mutant cells (Supplementary Fig. 5b), and inserting an additional copy of *ago1*$^+$ under its native promoter to restore wild-type protein levels did not rescue the silencing defect of *arb1*Δ and *arb2*Δ cells (data not shown). Moreover, *ago1*$^+$ overexpression failed to suppress a broad array of other mutations in components of the small RNA–mediated heterochromatin pathway (Supplementary Fig. 5c). Thus, overexpressed Ago1 acts specifically to circumvent a functional requirement for the ARC complex. To test the hypothesis that small-RNA loading constitutes the limiting process in *arb1*Δ cells that is overcome when Ago1 is highly overexpressed, we mutated a conserved leucine residue in the PAZ domain of Ago1 (L317), which in human Argonaute1 participates in securing the 3′ ends of guide small RNAs[42] and should therefore reduce the affinity of Ago1 for siRNAs. As expected, the *S. pombe ago1* L317A mutation caused a defect in the pericentromeric *otr1R::ura4*$^+$ silencing assay (Supplementary Fig. 6a). Nevertheless, a northern analysis of RNA associated with immunoprecipitated protein showed that Ago1 L317A was still loaded with *dg*-repeat siRNAs when overexpressed in wild-type cells (Supplementary Fig. 6b) and even when expressed at endogenous levels. Thus, this allele remained partly functional and, consistently with this, its overexpression complemented the deletion of *ago1*$^+$ in the *otr1R::ura4*$^+$ silencing assay (Fig. 6f). However,

unlike its wild-type counterpart, *ago1* L317A did not suppress the loss of silencing in *arb1*Δ cells. Thus, although overexpressed Ago1 can suppress the silencing defect of *arb1*Δ cells, this suppression requires its intact affinity for small RNAs, which is not necessary for silencing by overexpressed Ago1 when Arb1 is present. This observation lends further support to the idea that silencing is impaired in cells lacking Arb1 specifically because of a disruption in Argonaute loading. Together, our results demonstrate that small-RNA loading onto Argonaute, a critical step in RNA interference–mediated heterochromatin formation, is mediated by Arb1.

DISCUSSION

In this study, we have elucidated the role of the ARC complex in small RNA–dependent heterochromatin assembly. Our data reveal that loading of Argonaute with small-RNA molecules universally requires ARC subunit Arb1 unless Argonaute is vastly overexpressed. Our results also identify small-RNA loading as a critical event that enables Argonaute to assemble into RITS, a GW protein–containing effector complex. We propose that this ordered assembly mechanism has evolved to prevent the premature assembly of Argonautes lacking small-RNA guides into nonfunctional GW-protein complexes, which could engage in unproductive interactions with downstream silencing factors. These findings carry broad implications for the diversity of organisms in which small RNA–dependent silencing mechanisms rely on the physical association of Argonaute with a conserved GW-motif protein.

An Argonaute small RNA–loading complex in *S. pombe*

Rather than automatically binding available small RNAs, Argonautes must actively be loaded with their guides by associated factors. The loading machinery has been studied best in humans and *Drosophila*, in which the respective double-stranded RNA–binding proteins TRBP and R2D2 orchestrate the transfer of duplex small RNAs from the Dicer enzyme that generates them into the Argonaute protein[50–52]. We have previously noted that Arb1 and Arb2 apparently lack double-stranded RNA–binding domains and fail to associate detectably with Dcr1 (refs. 10,13). Nevertheless, the results in this study clearly identify an Arb1–Ago1 module as the siRNA-loading apparatus in *S. pombe* because only ARC, not RITS, binds duplex small RNAs *in vitro*, and all signatures of Argonaute-bound small RNAs vanish in *arb1*Δ cells.

In contrast, the molecular function of the ARC subunit Arb2 remains undefined. Cells lacking Arb2 contain an Ago1–Arb1 subcomplex, which, when isolated, exhibits duplex siRNA–loading activity *in vitro*. Therefore, we have excluded a direct biochemical role for Arb2 in loading small-RNA duplexes onto Ago1. We speculate that Arb2 may be required for correct subcellular localization of the Arb1–Ago1 heterodimer, so that Ago1 in *arb2*Δ cells binds small RNAs but does not encounter Tas3.

GW proteins as sensors of Argonaute loading

Our results underscore the importance of small-RNA loading in licensing Argonautes for association with GW-protein effectors. In the most thorough investigation to date of the

recognition of an Argonaute by a GW protein, Till *et al.*[27] observed a striking concordance between the residues in human Argonaute2 required for TNRC6B binding *in vitro* and those predicted from earlier structural work to secure the 5′-monophosphorylated 5′-terminal nucleotide of a guide RNA[41]. Although RNA may not be necessary to observe the interaction at the high protein concentrations used *in vitro*, the results suggest that GW proteins may recognize a region of Argonaute whose conformation is modulated by RNA binding *in vivo*. Corroborating the conclusions of early experiments with truncated *Drosophila* proteins[33], a recent crystal structure of human Argonaute2 with free tryptophan suggests that GW motifs may in fact bind to a region in the PIWI domain located at a site proximal to, but distinct from, the RNA 5′ end–binding site[43]. Conspicuously, residues of Argonaute2 belonging to the tryptophan-binding pockets resolved by Schirle and Macrae[43], such as R583, I592, R647, F653 and K660, are also critical for the *in vitro* interaction between Argonaute2 and TNRC6B[27].

We propose that GW proteins act as sensors of small-RNA loading onto Argonaute proteins. Engagement of Argonaute with a small-RNA guide, particularly at its 5′ end, may propagate a critical conformational change to the GW-binding site in the PIWI domain and trigger a permissive state for GW-protein association. We have shown here that, consistently with this model, the *S. pombe* GW protein Tas3 does not associate with the unloaded Argonautes Ago1 F276A R773E and Ago1 R773E *in vivo*. Importantly, the mutant Ago1 proteins still associate with Arb1 at near-wild-type levels, thus indicating that they remain competent to undergo protein-protein interactions. Finally, our observation that wild-type Ago1 fails to assemble into RITS in the absence of Arb1 lends further support to the idea that GW proteins detect the loading state of Argonautes. In apparent contradiction to the model of GW proteins as small-RNA sensors, two previous studies have identified Argonaute mutants with defects in small-RNA binding that still associate with GW proteins in human and *Drosophila* cells[36,37]. However, these studies were performed with overexpressed proteins, and it is unclear whether the observed interactions persist at physiological protein concentrations. And indeed, more exhaustive analyses with *Drosophila* AGO1 have revealed that mutants deficient in small-RNA loading consistently fail to associate with GW182 in cells but that certain mutants that do not associate with GW182 still load small RNAs[53,54]. Together with our data, these findings suggest that GW-protein docking occurs downstream of the programming of Argonaute with a small RNA.

Safeguards in the assembly of GW silencing complexes

This mechanism of sensing small-RNA loading may have evolved in order to preserve GW proteins from wasteful interactions with unguided Argonautes. Because GW proteins form a critical link between sequence-specific small-RNA signals and the machineries that carry out gene silencing, such as the CCR4–NOT deadenylase complex in metazoans and the CLRC H3K9-methyltransferase complex in *S. pombe*[17,28–30], their availability is expected to be important for ensuring the efficiency of silencing. In this model, association of Tas3 and other GW proteins with unloaded Argonautes would be deleterious because these nonfunctional complexes could compete with small RNA–programmed Argonautes for interactions with downstream factors. Thus, by rejecting unloaded Argonaute molecules, GW proteins would prevent them from acting as poisons that would make silencing systems

less responsive to small RNA–specificity signals (Fig. 7). In *S. pombe*, the slicer mutant Ago1 D580A illustrates this type of danger: although it is loaded with small RNAs, these remain double-stranded, and the mutant Argonaute therefore renders the RITS complex inactive. This produces a dominant-negative phenotype upon overexpression[13] (Supplementary Fig. 7), thus suggesting that the exclusion of immature Argonautes from silencing complexes is imperative for proper functioning of the pathway.

ONLINE METHODS

Strain construction

S. pombe strains used in this study are described in Supplementary Table 2 and were generated with a PCR-based gene-targeting strategy[55]. All gene deletions were made by replacement of the coding region (ATG to stop) with a drug-resistance cassette. The N-terminally tagged 3×Flag-*ago1* allele at the native *ago1*$^+$ locus was made by concurrent insertion of a drug-resistance cassette 808 bp upstream of the ATG and a 3×Flag coding sequence immediately upstream of the ATG (ref. 13). The N-terminally tagged TAP-*arb1* allele at the native *arb1*$^+$ locus was made by concurrent insertion of a drug-resistance cassette 560 bp upstream of the ATG and a TAP coding sequence immediately upstream of the ATG. The ectopic *trp1*$^+$::3×Flag-*ago1* wild-type and mutant alleles were generated as shown in Supplementary Figure 2a.

Coimmunoprecipitation and western blotting

Coimmunoprecipitations and western blots were carried out as previously described[12]. Rabbit IgG (Sigma) was used to prepare IgG-conjugated Dynabeads from Invitrogen Dynabeads M270 Epoxy according to the manufacturer's instructions. Antibodies used were peroxidase anti-peroxidase soluble complex (Sigma P-1291), 1:10,000 dilution; Flag M2-peroxidase (HRP) mouse monoclonal antibody (Sigma A-8592), 1:5,000 dilution; Anti–β-actin antibody (Abcam 8224), 1:2,500 dilution; and custom anti-Swi6 antisera (Covance), 1:5,000. Anti-Swi6 is validated in Supplementary Figure 5a, and validation information for all other antibodies used is provided on their respective manufacturers' websites.

Protein affinity purification and mass spectrometry

3×Flag-Ago1 was purified from 1-l cultures grown to a density of ~2.5 × 10^7 cells/ml. Anti-Flag beads were prepared as follows, with 37 µl Protein G Dynabeads per sample (Invitrogen). Beads were washed twice with 1 ml Tris-buffered saline (50 mM Tris-HCl, pH 7.5, and 150 mM NaCl) and then twice with 1 ml lysis buffer (20 mM HEPES, pH 7.6, 100 mM NaCl, 5 mM $MgCl_2$, 1 mM EDTA, 10% glycerol, 0.25% Triton X-100, 0.5 mM DTT, 1 mM PMSF and Roche cOmplete EDTA-free protease-inhibitor cocktail). 9.25 µl anti-Flag M2 antibody per sample (Sigma) was added and incubated in 200 µl total volume of lysis buffer per sample with rotation overnight at 4 °C. Anti-Flag beads were cross-linked by two washes with 1 ml 0.2 M sodium borate, pH 9; incubation in 300 µl per sample of 0.2 M sodium borate, pH 9, containing 4 mg/ml dimethyl pimelimidate, for 30 min at room temperature; two washes with 1 ml 0.2 M ethanolamine-HCl, pH 8; incubation in 300 µl per sample of 0.2 M ethanolamine-HCl, pH 8, for 1 h 30 min; and finally three washes with 1 ml lysis buffer. Aliquots of 0.4 g of cells were resuspended in 0.4 ml lysis buffer in 2-ml tubes

and lysed with 1 ml acid-washed 0.5-mm glass beads per tube with four cycles of 45 s at 5,000 r.p.m. on a MagNA Lyser Instrument (Roche). Extracts were cleared by centrifugation for 15 min at 16,100*g* and were incubated with anti-Flag beads for 3 h at 4 °C. Beads were washed four times with 1 ml lysis buffer, and protein was eluted from beads by incubation in 0.5 ml 0.5 M NH_4OH for 20 min at 37° with shaking. Sixteen percent of each eluate was analyzed by silver stain (Pierce) to confirm specific enrichment of 3×Flag-Ago1, and 80 percent was analyzed by MS carried out in the Taplin Biological Mass Spectrometry Facility (Harvard Medical School).

Total RNA and total small-RNA Isolation

Total RNA was isolated with the hot phenol method[56]. Total small RNAs for northern blots were recovered with the mirVana miRNA Isolation Kit (Ambion) according to the manufacturer's instructions (Fig. 2b). Alternatively, total small RNAs were recovered by size-fractionation of total RNA as previously described[57] (Fig. 6d). For RT-PCR assays, total RNA was further purified with the RNeasy Mini kit (Qiagen), according to the protocol for RNA cleanup provided in the manufacturer's handbook, and then treated with RNase-free DNase I (Roche), 25 U for 50 μg RNA in each of two successive reactions performed for 30 min at 37 °C.

Isolation of protein-associated RNA for northern blots and small-RNA libraries

Tas3-TAP and TAP-Arb1 were purified from cultures of 3–6 l grown to a density of ~4 × 10^7 cells/ml. Cells were resuspended in 1 ml extraction buffer (10 mM Tris HCl, pH 8, 350 mM NaCl, 10% glycerol, 0.1% NP-40, 1 mM DTT, 1 mM PMSF and Roche cOmplete EDTA-free protease-inhibitor cocktail) per 1 g cells. Extracts were prepared by 11 10-s cycles of bead-beating in a Biospec bead-beater (model no. 1107900) with an 80-ml-capacity chamber, then cleared by centrifugation at 16,100*g* for 15 min. Supernatants were incubated in two 15-ml tubes with 250 μl prewashed IgG Sepharose 6 Fast Flow (GE Healthcare) for 3 h at 4 °C. Resin was then washed four times with 3 ml extraction buffer and treated with 2% SDS in 300 μl extraction buffer for 10 min at 65 °C. RNA was isolated by phenol/chloroform extraction. Wild-type or mutant 3×Flag-Ago1 for small-RNA sequencing was purified from cultures of 6 l grown to a density of 2 × 10^7 to 3 × 10^7 cells/ml. Cells were resuspended in 1 ml lysis buffer (20 mM HEPES, pH 7.6, 100 mM NaCl, 5 mM $MgCl_2$, 1 mM EDTA, 10% glycerol, 0.25% Triton X-100, 0.5 mM DTT, 1 mM PMSF and Roche cOmplete EDTA-free protease-inhibitor cocktail) per 5 g cells and frozen dropwise in liquid nitrogen. Frozen material was ground into a powder at liquid-nitrogen temperatures in a Retsch Cryomill (3 × 3 min at 30 Hz). Anti-Flag beads were prepared as follows, with 300 μl Protein G Dynabeads per sample (Invitrogen). Beads were washed with lysis buffer, and 45 μl anti-Flag M2 antibody per sample (Sigma) was added and incubated with rotation. Meanwhile, extracts were prepared by resuspension of frozen cell powders in 2 ml lysis buffer per 3 g powder and centrifugation of the thawed suspension for 15 min at 16,100*g*. Extracts were incubated with anti-Flag beads for 2 h at 4 °C. Beads were washed four times with 1 ml lysis buffer, and then RNA was eluted by treatment with Proteinase K (80 U/ml final concentration in 30 mM Tris-HCl, pH 8) for 30 min at 37 °C; this was followed by incubation in 2% SDS for 10 min at 65 °C and extraction with phenol/chloroform. For northern blots, 3×Flag-Ago1 was isolated similarly but from cultures of 3 l

grown to a density of ~3 × 10^7 cells/ml (*ago1*$^+$ promoter) or 1 l grown to a density of ~6 × 10^7 cells/ml (overexpressed) and with 70 μl packed EZview Red Anti-Flag M2 Affinity Gel (Sigma) per sample.

Northern blots

Northern blots were performed as previously described[57] with total small RNAs or RNA isolated from Tas3-TAP, TAP-Arb1 or 3×Flag-Ago1 affinity purifications (described above). Oligonucleotide probes are listed in Supplementary Table 3.

Small-RNA libraries

RNA was isolated from Tas3-TAP, TAP-Arb1 or 3×Flag-Ago1 affinity purifications (described above). Small RNAs were size-selected (18–28 nt) by PAGE and then were used for library construction as previously described[39]. Tas3-TAP– and TAP-Arb1–associated small-RNA libraries were each sequenced in individual lanes on an Illumina GAIIx instrument. 3×Flag-Ago1– associated small-RNA libraries carried barcodes added with oligonucleotides shown in Supplementary Table 3 and were sequenced as a mixture in a single lane on an Illumina HiSeq instrument.

Analysis of small-RNA sequences

Small-RNA sequencing data were processed and analyzed with custom Perl and Python scripts, which are available upon request. The genome sequence and annotation were obtained from PomBase (http://www.pombase.org/). Reads that lacked the 3′ cloning linker, were shorter than 17 nt, or contained ten or more consecutive adenosines were excluded. The remaining reads were aligned to the *S. pombe* genome with NovoAlign (http://www.novocraft.com/). A maximum of either one mismatch or one insertion or deletion of one nucleotide was tolerated. Reads mapping to multiple locations were randomly assigned. The final numbers of aligned reads for each library are displayed in Supplementary Table 1. Tracks were generated with Integrative Genomics Viewer (IGV) (http://www.broadinstitute.org/igv/).

Protein immobilization for *in vitro* binding assays

IgG-conjugated Dynabeads were prepared from Dynabeads M270 Epoxy (Invitrogen) according to the manufacturer's instructions with rabbit IgG (Sigma). Anti-Flag beads were prepared as follows, with 25 μl Protein G Dynabeads per sample (Invitrogen). Beads were washed with lysis buffer (20 mM HEPES, pH 7.6, 100 mM NaCl, 5 mM $MgCl_2$, 1 mM EDTA, 10% glycerol, 0.25% Triton X-100, 0.5 mM DTT, 1 mM PMSF and Roche cOmplete EDTA-free protease-inhibitor cocktail). 6.25 μl anti-Flag M2 antibody per sample (Sigma) was added and incubated in 120 μl total volume of lysis buffer per sample with rotation. Tas3-TAP and TAP-Arb1 were purified from cultures of 6 l, and 3×Flag-Ago1 was purified from cultures of 3 l, all grown to a density of ~3 × 10^7 cells/ml. Cells were resuspended in 1 ml lysis buffer per 5 g cells and frozen dropwise in liquid nitrogen. Frozen material was ground into a powder at liquid-nitrogen temperatures in a Retsch Cryomill (3 × 3 min at 30 Hz). Extracts were prepared by resuspension of frozen cell powders in 2 ml lysis buffer per 3 g powder and centrifugation of the thawed suspension for 15 min at 16,100*g*.

Extracts containing Tas3-TAP or TAP-Arb1 and control extracts lacking TAP-tagged protein were incubated with 50 µl IgG-conjugated Dynabeads (corresponding to 0.375 mg original dry beads) for 2 h at 4 °C. Extracts containing 3×Flag-Ago1 and control extracts containing untagged Ago1 were incubated with 25 µl anti-Flag beads for 2 h at 4 °C. Beads were washed four times with 1 ml lysis buffer and resuspended in lysis buffer containing 50 µl (TAP samples) or 25 µl (Flag samples) of 0.1 mg/ml BSA. For the experiment in Supplementary Figure 4c–e, the lysis buffer was modified to contain 40 mM NaCl instead of 100 mM.

In vitro binding assays

Tas3-TAP, TAP-Arb1 and 3×Flag-Ago1 were immobilized on magnetic beads from *S. pombe* extracts, and mock beads were prepared in parallel by incubation with control extracts lacking tagged proteins (described above). Aliquots of 4 µl beads for each protein sample were washed with 1 ml wash buffer (30 mM HEPES, pH 7.6, 40 mM KOAc, 5 mM $Mg(OAc)_2$, 10% glycerol and 5 mM DTT) and then resuspended in binding buffer (30 mM HEPES, pH 7.6, 40 mM KOAc, 5 mM $Mg(OAc)_2$, 0.1 mg/ml BSA, 5 mM DTT and 2 U/µl RNasin (Promega)) containing 0.4 nM single-stranded or duplex small RNA (sequences in Supplementary Table 3) 5′-end-labeled with polynucleotide kinase and a five-fold molar excess of [γ-^{32}P]ATP. After incubation for 1 h 30 min at room temperature, beads were washed four times with 1 ml wash buffer. To elute RNAs, beads were resuspended in 8 µl proteinase K reaction buffer (80 U/ml proteinase K (NEB) in 30 mM Tris-HCl, pH 8) and incubated 30 min at 37 °C; 8 µl of formamide was then added, and samples were incubated 2 min at 95 °C. RNAs were visualized by denaturing PAGE and autoradiography and quantified by densitometry with Quantity One software (Bio-Rad).

Growth assays

Cells were grown to saturation and diluted serially ten-fold (except for thiabendazole growth assays, which were diluted serially five-fold) so that the highest-density spot contained 1.3×10^5 cells. Nonselective plates contained Edinburgh Minimal Medium with all standard supplements (Sunrise Science Products) except leucine to ensure maintenance of the transformed plasmids (Supplementary Table 4). Selective plates additionally contained 1 g/L 5-fluoroorotic acid or 17 mg/L thiabendazole. Low-adenine plates contained 10 mg/L adenine.

Reverse transcription

cDNA was prepared with transcript-specific oligonucleotide primers (Supplementary Table 3) and Superscript III Reverse Transcriptase (Invitrogen). *dg* and *dh* reactions contained primers to reverse-transcribe both strands. *act1*$^+$ reactions contained only a primer to reverse-transcribe forward transcripts. A mock reaction without reverse transcriptase was performed for every sample.

Chromatin immunoprecipitation

ChIP was performed as previously described[58]. For each sample, 30 µl of Protein A Dynabeads (Invitrogen) and 2 µg anti–histone H3-dimethyl K9 (Abcam 1220) antibody were

used. Validation information for anti–histone-H3-dimethyl K9 is provided on the manufacturer's website.

Quantitative PCR

DNA, cDNA or mock cDNA (–reverse transcriptase) was amplified with Taq polymerase with oligonucleotide primers described in Supplementary Table 3 in the presence of SYBR Green in an Applied Biosystems 7900HT Fast Real-Time PCR instrument. A standard serial dilution was included for each primer set on each plate in order to determine amplification efficiency and calculate precise relative quantities among samples. All mock cDNA reactions generated less than one one-thousandth (*act1*$^{+}$) or one-third (*dg*, *dh*) the corresponding +reverse transcriptase signal.

Supplementary Material

Refer to Web version on PubMed Central for supplementary material.

Acknowledgments

We thank members of the Moazed laboratory for helpful discussions; E. Gerace, M. Halic, N. Iglesias and J. Xiol for advice on protocols; M. Halic and R. Yu for scripts and advice on bioinformatic analysis; C. Centrella for technical assistance; and E. Egan, N. Iglesias, R. Jain, J. Xiol and R. Yu for critical reading of the manuscript. This work was supported by the US National Science Foundation Graduate Research Fellowship Program (D.H.) and the US National Institutes of Health grant R01 GM072805 (D.M.). D.M. is supported as a Howard Hughes Medical Institute Investigator. D.H. dedicates this paper to the memory of his beloved father, George Holoch, who died on 9 April 2013.

References

1. Ghildiyal M, Zamore PD. Small silencing RNAs: an expanding universe. Nat Rev Genet. 2009; 10:94–108. [PubMed: 19148191]
2. Malone CD, Hannon GJ. Small RNAs as guardians of the genome. Cell. 2009; 136:656–668. [PubMed: 19239887]
3. Moazed D. Small RNAs in transcriptional gene silencing and genome defence. Nature. 2009; 457:413–420. [PubMed: 19158787]
4. Olovnikov I, Chan K, Sachidanandam R, Newman DK, Aravin AA. Bacterial Argonaute samples the transcriptome to identify foreign DNA. Mol Cell. 2013; 51:594–605. [PubMed: 24034694]
5. Hutvagner G, Simard MJ. Argonaute proteins: key players in RNA silencing. Nat Rev Mol Cell Biol. 2008; 9:22–32. [PubMed: 18073770]
6. Jinek M, Doudna JA. A three-dimensional view of the molecular machinery of RNA interference. Nature. 2009; 457:405–412. [PubMed: 19158786]
7. Meister G. Argonaute proteins: functional insights and emerging roles. Nat Rev Genet. 2013; 14:447–459. [PubMed: 23732335]
8. Hammond SM, Bernstein E, Beach D, Hannon GJ. An RNA-directed nuclease mediates post-transcriptional gene silencing in *Drosophila* cells. Nature. 2000; 404:293–296. [PubMed: 10749213]
9. Verdel A, et al. RNAi-mediated targeting of heterochromatin by the RITS complex. Science. 2004; 303:672–676. [PubMed: 14704433]
10. Colmenares SU, Buker SM, Buhler M, Dlakić M, Moazed D. Coupling of double-stranded RNA synthesis and siRNA generation in fission yeast RNAi. Mol Cell. 2007; 27:449–461. [PubMed: 17658285]
11. Reinhart BJ, Bartel DP. Small RNAs correspond to centromere heterochromatic repeats. Science. 2002; 297:1831. [PubMed: 12193644]

12. Yu R, Jih G, Iglesias N, Moazed D. Determinants of heterochromatic siRNA biogenesis and function. Mol Cell. 2014; 53:262–276. [PubMed: 24374313]
13. Buker SM, et al. Two different Argonaute complexes are required for siRNA generation and heterochromatin assembly in fission yeast. Nat Struct Mol Biol. 2007; 14:200–207. [PubMed: 17310250]
14. Matranga C, Tomari Y, Shin C, Bartel DP, Zamore PD. Passenger-strand cleavage facilitates assembly of siRNA into Ago2-containing RNAi enzyme complexes. Cell. 2005; 123:607–620. [PubMed: 16271386]
15. Rand TA, Petersen S, Du F, Wang X. Argonaute2 cleaves the anti-guide strand of siRNA during RISC activation. Cell. 2005; 123:621–629. [PubMed: 16271385]
16. Bayne EH, et al. Stc1: a critical link between RNAi and chromatin modification required for heterochromatin integrity. Cell. 2010; 140:666–677. [PubMed: 20211136]
17. Gerace EL, Halic M, Moazed D. The methyltransferase activity of Clr4Suv39h triggers RNAi independently of histone H3K9 methylation. Mol Cell. 2010; 39:360–372. [PubMed: 20705239]
18. Hong EJE, Villén J, Gerace EL, Gygi SP, Moazed DA. Cullin E3 ubiquitin ligase complex associates with Rik1 and the Clr4 histone H3-K9 methyltransferase and is required for RNAi-mediated heterochromatin formation. RNA Biol. 2005; 2:106–111. [PubMed: 17114925]
19. Volpe TA, et al. Regulation of heterochromatic silencing and histone H3 lysine-9 methylation by RNAi. Science. 2002; 297:1833–1837. [PubMed: 12193640]
20. Zhang K, Mosch K, Fischle W, Grewal SIS. Roles of the Clr4 methyltransferase complex in nucleation, spreading and maintenance of heterochromatin. Nat Struct Mol Biol. 2008; 15:381–388. [PubMed: 18345014]
21. Bernard P, et al. Requirement of heterochromatin for cohesion at centromeres. Science. 2001; 294:2539–2542. [PubMed: 11598266]
22. Ellermeier C, et al. RNAi and heterochromatin repress centromeric meiotic recombination. Proc Natl Acad Sci USA. 2010; 107:8701–8705. [PubMed: 20421495]
23. Probst AV, Dunleavy E, Almouzni G. Epigenetic inheritance during the cell cycle. Nat Rev Mol Cell Biol. 2009; 10:192–206. [PubMed: 19234478]
24. Azevedo J, Cooke R, Lagrange T. Taking RISCs with Ago hookers. Curr Opin Plant Biol. 2011; 14:594–600. [PubMed: 21807551]
25. Braun JE, Huntzinger E, Izaurralde E. The role of GW182 proteins in miRNA-mediated silencing. Adv Exp Med Biol. 2013; 768:147–163. [PubMed: 23224969]
26. El-Shami M, et al. Reiterated WG/GW motifs form functionally and evolutionarily conserved ARGONAUTE-binding platforms in RNAi-related components. Genes Dev. 2007; 21:2539–2544. [PubMed: 17938239]
27. Till S, et al. A conserved motif in Argonaute-interacting proteins mediates functional interactions through the Argonaute PIWI domain. Nat Struct Mol Biol. 2007; 14:897–903. [PubMed: 17891150]
28. Braun JE, Huntzinger E, Fauser M, Izaurralde E. GW182 proteins directly recruit cytoplasmic deadenylase complexes to miRNA targets. Mol Cell. 2011; 44:120–133. [PubMed: 21981923]
29. Chekulaeva M, et al. miRNA repression involves GW182-mediated recruitment of CCR4–NOT through conserved W-containing motifs. Nat Struct Mol Biol. 2011; 18:1218–1226. [PubMed: 21984184]
30. Fabian MR, et al. miRNA-mediated deadenylation is orchestrated by GW182 through two conserved motifs that interact with CCR4–NOT. Nat Struct Mol Biol. 2011; 18:1211–1217. [PubMed: 21984185]
31. Partridge JF, et al. Functional separation of the requirements for establishment and maintenance of centromeric heterochromatin. Mol Cell. 2007; 26:593–602. [PubMed: 17531816]
32. Pontier D, et al. NERD, a plant-specific GW protein, defines an additional RNAi-dependent chromatin-based pathway in *Arabidopsis*. Mol Cell. 2012; 48:121–132. [PubMed: 22940247]
33. Behm-Ansmant I, et al. mRNA degradation by miRNAs and GW182 requires both CCR4:NOT deadenylase and DCP1:DCP2 decapping complexes. Genes Dev. 2006; 20:1885–1898. [PubMed: 16815998]

34. Baillat D, Shiekhattar R. Functional dissection of the human TNRC6 (GW182-related) family of proteins. Mol Cell Biol. 2009; 29:4144–4155. [PubMed: 19470757]
35. Giner A, Lakatos L, García-Chapa M, López-Moya JJ, Burgyán J. Viral protein inhibits RISC activity by argonaute binding through conserved WG/GW motifs. PLoS Pathog. 2010; 6:e1000996. [PubMed: 20657820]
36. Eulalio A, Helms S, Fritzsch C, Fauser M, Izaurralde E. A C-terminal silencing domain in GW182 is essential for miRNA function. RNA. 2009; 15:1067–1077. [PubMed: 19383769]
37. Liu J, Valencia-Sanchez MA, Hannon GJ, Parker R. MicroRNA-dependent localization of targeted mRNAs to mammalian P-bodies. Nat Cell Biol. 2005; 7:719–723. [PubMed: 15937477]
38. Woolcock KJ, et al. RNAi keeps Atf1-bound stress response genes in check at nuclear pores. Genes Dev. 2012; 26:683–692. [PubMed: 22431512]
39. Halic M, Moazed D. Dicer-independent primal RNAs trigger RNAi and heterochromatin formation. Cell. 2010; 140:504–516. [PubMed: 20178743]
40. Marasovic M, Zocco M, Halic M. Argonaute and Triman generate Dicer-independent priRNAs and mature siRNAs to initiate heterochromatin formation. Mol Cell. 2013; 52:173–183. [PubMed: 24095277]
41. Ma JB, et al. Structural basis for 5′-end-specific recognition of guide RNA by the *A. fulgidus* Piwi protein. Nature. 2005; 434:666–670. [PubMed: 15800629]
42. Ma JB, Ye K, Patel DJ. Structural basis for overhang-specific small interfering RNA recognition by the PAZ domain. Nature. 2004; 429:318–322. [PubMed: 15152257]
43. Schirle NT, MacRae IJ. The crystal structure of human Argonaute2. Science. 2012; 336:1037–1040. [PubMed: 22539551]
44. Iida T, Nakayama J, Moazed D. siRNA-mediated heterochromatin establishment requires HP1 and is associated with antisense transcription. Mol Cell. 2008; 31:178–189. [PubMed: 18657501]
45. Irvine DV, et al. Argonaute slicing is required for heterochromatic silencing and spreading. Science. 2006; 313:1134–1137. [PubMed: 16931764]
46. Martinez NJ, Gregory RI. Argonaute2 expression is post-transcriptionally coupled to microRNA abundance. RNA. 2013; 19:605–612. [PubMed: 23485552]
47. Smibert P, Yang JS, Azzam G, Liu JL, Lai EC. Homeostatic control of Argonaute stability by microRNA availability. Nat Struct Mol Biol. 2013; 20:789–795. [PubMed: 23708604]
48. Frank F, Sonenberg N, Nagar B. Structural basis for 5′-nucleotide base-specific recognition of guide RNA by human AGO2. Nature. 2010; 465:818–822. [PubMed: 20505670]
49. Bühler M, Spies N, Bartel DP, Moazed D. TRAMP-mediated RNA surveillance prevents spurious entry of RNAs into the *Schizosaccharomyces pombe* siRNA pathway. Nat Struct Mol Biol. 2008; 15:1015–1023. [PubMed: 18776903]
50. Gregory RI, Chendrimada TP, Cooch N, Shiekhattar R. Human RISC couples microRNA biogenesis and posttranscriptional gene silencing. Cell. 2005; 123:631–640. [PubMed: 16271387]
51. Liu Q, et al. R2D2, a bridge between the initiation and effector steps of the *Drosophila* RNAi pathway. Science. 2003; 301:1921–1925. [PubMed: 14512631]
52. Maniataki E, Mourelatos Z. A human, ATP-independent, RISC assembly machine fueled by pre-miRNA. Genes Dev. 2005; 19:2979–2990. [PubMed: 16357216]
53. Boland A, Huntzinger E, Schmidt S, Izaurralde E, Weichenrieder O. Crystal structure of the MID-PIWI lobe of a eukaryotic Argonaute protein. Proc Natl Acad Sci USA. 2011; 108:10466–10471. [PubMed: 21646546]
54. Eulalio A, Huntzinger E, Izaurralde E. GW182 interaction with Argonaute is essential for miRNA-mediated translational repression and mRNA decay. Nat Struct Mol Biol. 2008; 15:346–353. [PubMed: 18345015]
55. Bähler J, et al. Heterologous modules for efficient and versatile PCR-based gene targeting in *Schizosaccharomyces pombe*. Yeast. 1998; 14:943–951. [PubMed: 9717240]
56. Leeds P, Peltz SW, Jacobson A, Culbertson MR. The product of the yeast UPF1 gene is required for rapid turnover of mRNAs containing a premature translational termination codon. Genes Dev. 1991; 5:2303–2314. [PubMed: 1748286]

57. Bühler M, Verdel A, Moazed D. Tethering RITS to a nascent transcript initiates RNAi- and heterochromatin-dependent gene silencing. Cell. 2006; 125:873–886. [PubMed: 16751098]

58. Huang J, Moazed D. Association of the RENT complex with nontranscribed and coding regions of rDNA and a regional requirement for the replication fork block protein Fob1 in rDNA silencing. Genes Dev. 2003; 17:2162–2176. [PubMed: 12923057]

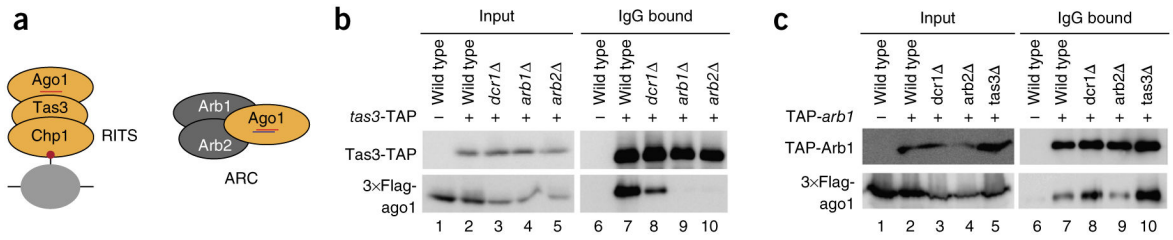

Figure 1.

ARC subunits Arb1 and Arb2 are required for RITS assembly. (**a**) Schematic illustrating the subunit composition of the RITS and ARC complexes. RITS is represented carrying a single-stranded small RNA (red line) and is bound via Chp1 to a nucleosome (gray) methylated (red dot) on H3K9, whereas ARC is shown loaded with a duplex small RNA (red and blue lines). (**b**) Western blot analysis of coimmunoprecipitation experiment to assay Tas3-Ago1 association in the indicated wild-type and mutant cells. Shown is one of two independent experiments. (**c**) Western blot analysis of coimmunoprecipitation experiment to assay Arb1–Ago1 association in the indicated wild-type and mutant cells. Supplementary Data Set 1 shows uncropped blot images for this figure.

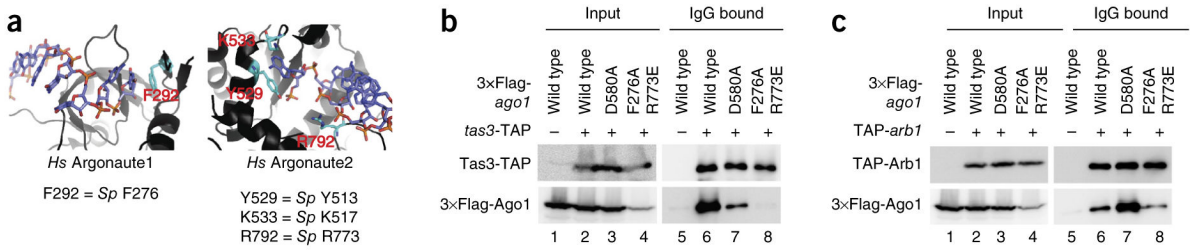

Figure 2.

Loading of small RNAs onto Ago1 is required for assembly of RITS but not ARC. (**a**) Views of the human (*Hs*) Argonaute1 PAZ domain[42] (left) and full-length Argonaute2 (ref. 43) (right), each in complex with a small RNA, illustrating the residues chosen for mutagenesis in the corresponding *S. pombe* Ago1 protein to abrogate small-RNA binding. Equivalent residues in *S. pombe* (*Sp*) Argonaute are indicated. (**b**) Western blot analysis of coimmunoprecipitation experiment to assay association of Tas3 with the indicated Ago1 proteins. Result was identical in a separate experiment substituting Ago1 F276A Y513A K517A for Ago1 F276A R773E (data not shown). (**c**) Western blot analysis of coimmunoprecipitation experiment to assay association of Arb1 with the indicated Ago1 proteins. Result was identical in a separate experiment substituting Ago1 F276A Y513A K517A for Ago1 F276A R773E (data not shown). Supplementary Data Set 1 shows uncropped blot images for this figure.

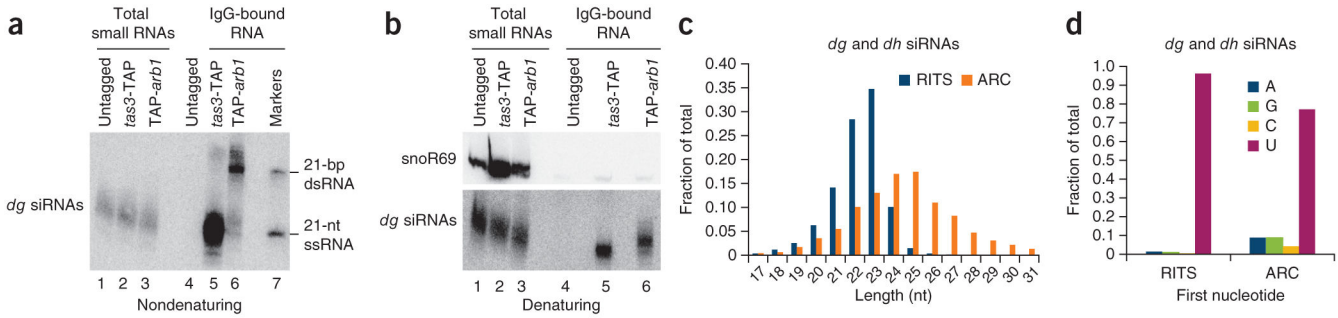

Figure 3.

ARC binds small RNAs *in vivo* that bear features of Dcr1-generated duplexes. (**a**,**b**) Non-denaturing (**a**) and denaturing (**b**) northern blot analyses of *dg* siRNAs contained in RITS- and ARC-complex purifications. Shown are total small-RNA fractions and separately prepared RNA extracted from one-step TAP purifications from cells of the indicated genotypes. **a** and **b** each represent an independent set of cell cultures. Supplementary Data Set 1 shows uncropped blot images. (**c**) Reads from high-throughput sequencing analysis of small RNAs copurifying with Tas3-TAP and TAP-Arb1 mapping to the *dg* and *dh* repeats, plotted according to their length. (**d**) Fraction of *dg* and *dh* reads beginning with each of the four nucleotides, shown for each complex.

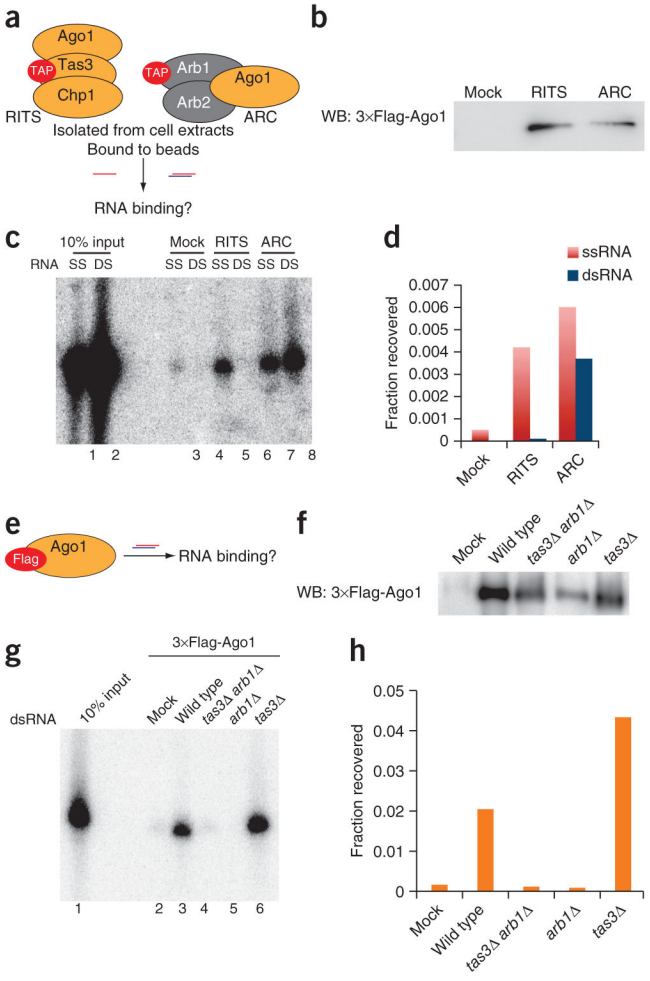

Figure 4.

Immunopurified Ago1 binds duplex small RNAs *in vitro* in an Arb1-dependent manner. (**a**) Schematic of *in vitro* RNA binding assay. Detailed description in main text. (**b**) Western blot (WB) showing relative abundance of 3×Flag-Ago1 in aliquots of beads equal to those used in the binding assay. (**c**) Phosphorimager scan of eluted RNAs after *in vitro* binding to immobilized complexes. Shown is one of two technical replicates. SS, single stranded; DS, double stranded. (**d**) Quantification by densitometry of the results in **c**. (**e**) Schematic of *in vitro* assay: similar to **a**–**d** but with 3×Flag-Ago1 instead of complexes. Detailed description in main text. (**f**) Western blot showing relative abundance of 3×Flag-Ago1 in aliquots equal to one-eighth of those used in the binding assay. (**g**) Phosphorimager scan of eluted RNAs after *in vitro* binding to immobilized 3×Flag-Ago1 purified from the indicated wild-type and mutant cells. dsRNA, double-stranded RNA. (**h**) Quantification by densitometry of the results shown in **g**. Supplementary Data Set 1 shows uncropped gel images for this figure.

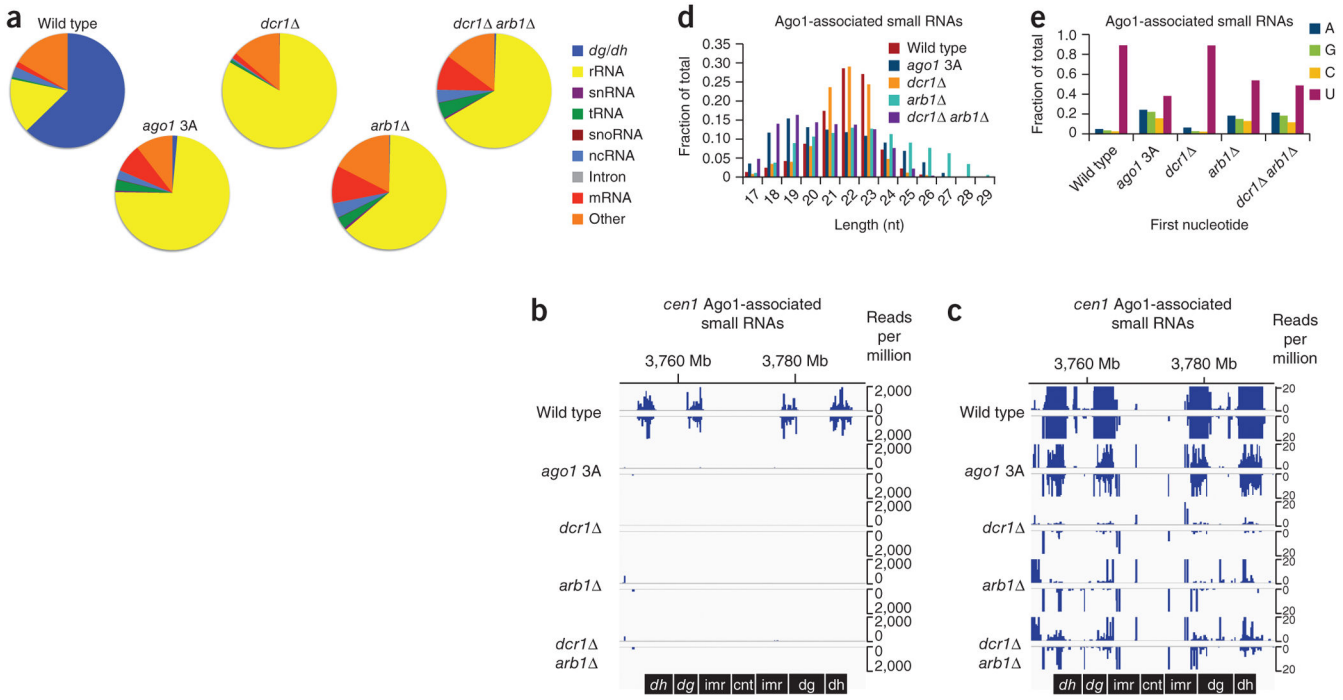

Figure 5.

Arb1 is required for all Ago1 small RNA–loading activity *in vivo*. (**a**–**e**) High-throughput sequencing analysis of small RNAs copurifying with wild-type 3×Flag-Ago1 in the indicated cells or with the loading mutant 3×Flag-Ago1 F276A Y513A K517A (Ago1 3A) from cells also bearing wild-type untagged *ago1*$^{+}$. (**a**) Reads are classified as shown in the legend on the right. *dg*/*dh*, *dg* and *dh*; snRNA, small nuclear RNA; snoRNA, small nucleolar RNA; ncRNA, noncoding RNA. (**b**,**c**) Tracks showing the normalized numbers of reads mapping to the *dg* and *dh* repeats flanking the centromere of chromosome 1 in each library. The two panels represent the same data plotted on different scales. (**d**) Histogram comparing the genome-wide read length distributions of each library. (**e**) The fraction of reads beginning with each nucleotide genome wide in each library.

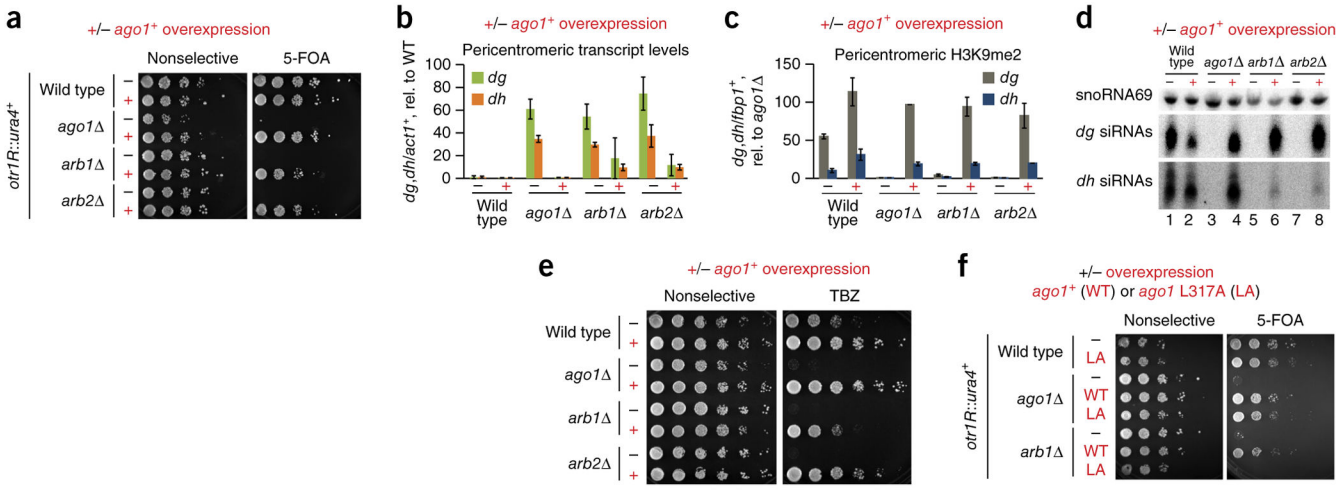

Figure 6.

ago1$^+$ overexpression partially suppresses silencing defect of *arb1*Δ and *arb2*Δ by overcoming the requirement for ARC in small-RNA loading. (**a**–**e**) Analysis of cells transformed with empty vector (−) or 3×Flag-*ago1* overexpression plasmid (red +). (**a**) Ten-fold serial dilutions of cells of the indicated genotypes carrying pericentromeric *ura4*$^+$ reporter gene *otr1R::ura4*$^+$, plated on the indicated medium. Shown is one of two independent sets of cell cultures. (**b**) Relative (rel.) levels of *dg* and *dh* transcripts measured by quantitative PCR with reverse transcription, normalized to *act1*$^+$ mRNA, with the mean for wild-type cells carrying the empty vector set to 1. Error bars, s.d. of three independent cell cultures. (**c**) Relative levels of dimethylated H3K9 (H3K9me2) measured at the *dg* and *dh* pericentromeric repeats by chromatin immunoprecipitation and quantitative PCR, normalized to the euchromatic *fbp1*$^+$ locus, with the mean for *ago1*Δ cells carrying the empty vector set to 1. Range bars represent two independent cell cultures. (**d**) Northern blot analysis of small RNAs isolated from total RNA by size-fractionation. Shown is one of two replicates performed with RNA isolated from independent sets of cell cultures. (**e**) Five-fold serial dilutions of wild type and the indicated mutant cells plated on the indicated media. TBZ, thiabendazole. (**f**) Ten-fold serial dilutions of *otr1R::ura4*$^+$ pericentromeric silencing reporter cells of the indicated genotypes transformed with empty vector (−) or plasmid for overexpression of the wild-type 3×Flag-*ago1* allele (red WT) or of the small RNA–loading mutant allele 3×Flag-*ago1* L317A (red LA) plated on the indicated medium. 5-FOA, 5-fluoroorotic acid.

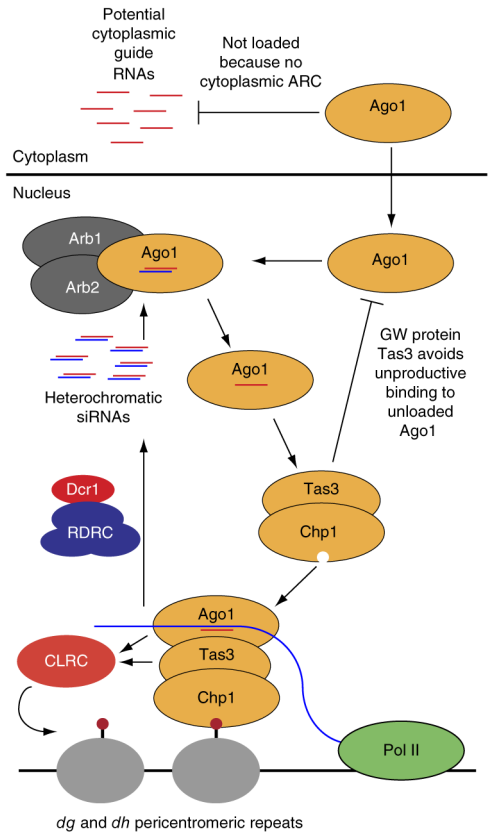

Figure 7.

Regulation of RITS-complex assembly by small-RNA loading onto Argonaute. The requirement for the nuclear complex ARC in loading Ago1 with small RNAs prevents Ago1 from binding guide RNAs in the cytoplasm and mediating post-transcriptional gene silencing. In the nucleus, Ago1 associates with Arb1 and Arb2, which enable its loading with heterochromatic duplex siRNAs generated by the RNA-dependent RNA polymerase complex (RDRC) and Dcr1. Small-RNA loading renders Ago1 competent for assembly into the RITS effector complex, whose sequence-specific recruitment to nascent transcripts synthesized by RNA polymerase II (Pol II) leads to CLRC-dependent methylation of H3K9 (red circles). The GW motif–containing RITS subunit Tas3 rejects unloaded Ago1, preventing unproductive interactions that would compromise silencing.